

# Effects of Different Parameters on Tool Tip Temperature and Force Components during Turning

Rahul Kshetri & Dr. Ajay

Department of Industrial & Production Engineering,  
G.B. Pant University of Agriculture & Technology, Pantnagar- 263145  
*rahulkshetricot@gmail.com*

**Abstract**— This communication is based on the effects of machining parameter on components of forces and tool tip temperature. In present work cutting speed, feed rate, cutting edge angle and rake angle have been selected as independent parameters. Cemented carbide inserts Komet WCMT 040303 FR ES in grade of P25M and AISI 1040 steel hardened at HRC 40 have been taken as tool and workpiece respectively. During machining operation, the tool experiences three kind of forces, while removing unwanted material from the work piece. These components of forces and high cutting speed cause temperature generation at the tool tip. The comparison of calculated and experimental values of temperatures using data from literature survey has been presented in this paper along with their trends for different input parameters.

**Keywords**- Machining, Force components, Tool tip temperature

**Symbols**- Rake angle= ( $\gamma$ ), Cutting edge angle=  $\chi$ ,  $F_c$  Cutting Force (N),  $F_f$  =Feed force (N),  $F_t$ = Thrust Force(N)

## 1. INTRODUCTION

Presented literature covers maximum possible position of cutting edge angle and rake angle during the turning operation and their effects on components of forces and tool tip temperature by selecting input parameters e.g cutting speed and feed rate. This work is an attempt to find out all the effects of input independent parameters on the dependent parameters viz components of cutting forces and tool tip temperature, have been shown with the help of graphs. Lima et al. [1-3] concluded the effects of cutting speed, feed rate and depth of cut on surface roughness and cutting forces in hardened AISI 4340 high strength low alloy steel and AISI D2 cold work tool steel materials. Chou and Song [4] reported that rake angle ( $-25^\circ$ ) with a large nose radius enhanced the value of force components who is helpful for batter surface finishing during hard turning of AISI 52100 steel with ceramic tool. Another explanation made by Astakhov [5] bounded up the dominance of thrust force to the spring back of the machined surface. Bouacha et al. [6] investigated thrust force evolution and considered that hardness of work piece is a function of thrust force. Kurt and Seker [7] studied and concluded that the thrust force has to be influences by the chamfer angle of PCBN insert a compared to tangential component. Ultimately, the conclusion has been drawn that is at low cutting speed magnitude of force would be high and must be the

formation of built up edge BUE which is causes increases the dynamic forces, and excessive chipping causes fracture of the brittle ceramic tool. It has been well claimed that the chip was formed in the shear plane and was shaped in the sliding plane. Therefore, the shear angle is a characteristic variable and depends on cleaving/wedge angle and friction. The contribution of cutting forces and temperature to the primary shear zone, chamfer and sticking, and sliding zones are expressed as a function of unknown shear angle, and known friction constants on the rake face and temperature modified flow stress in each zone [8].

## 2. METHODOLOGY

In presented work, effects of force components and tool tip temperature with different combinations of other parameters have been presented in the form of graphs. Table.1 represents all the data of cutting forces, tool tip temperature (calculated and experimental) by taking input parameters as rake angle, cutting edge angle and feed rate. The data for this work has been taken from literature [1].

### 2.1 Effects of Cutting Speed on Tool Tip Temperature

The graphs in between tool tip temperature (experimental and calculated) and speed (m/min) for constant cutting edge angle ( $\chi=90^\circ$ ) and variable rake angles ( $\gamma = 0^\circ, 6^\circ, 12^\circ, 20^\circ$ ) have been shown in Fig.1 to 4. As the rake angle increases, the tool tip temperature increases with increasing cutting speed.

The components of forces, tool tip temperature for different speed are given in Table.2. Effects of force components and tool tip temperature calculated and measured at different combination of other parameters mentioned below are presented in the form of graph. Table.2 represent all the data of cutting forces tool tip temperature (calculated and experimental ) by taking input parameters as rake angle, cutting edge angle and cutting speed data of [2].

According to trends of graph, experimental and calculated values shown in Fig 5 to 8 it have been very clear tool tip temperature increases their value with increasing cutting speed and temperature reaches their maximum value of tool tip temperature for 45° cutting edge angle at maximum speed and as soon as

the value of cutting edge angle reaches 90° value of tool tip temperature reaches their minimum value.

Variation of temperature with respect to feed for constant rake has been calculated as well as measured by experiment, and depicted in graph from fig 13 to 16. It has been very clear that as the value of feed increases, the tool tip temperature decreases. And with increasing cutting edge angle, the value of tool tip temperature decreased. As the cutting edge angle reaches maximum value 90°, the value of tool tip temperature would be minimum as compared to other values of cutting edge angle

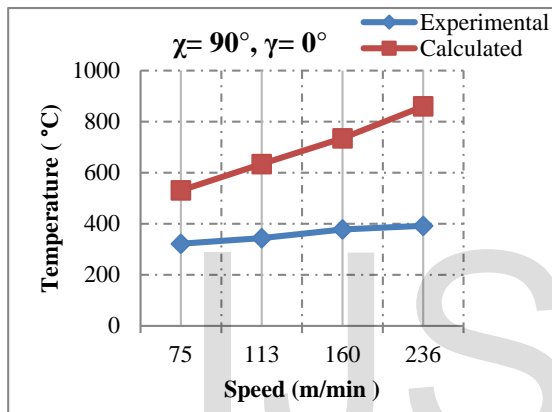


Fig. Experimental and calculated value for  $\chi = 90^\circ, \gamma = 0^\circ$

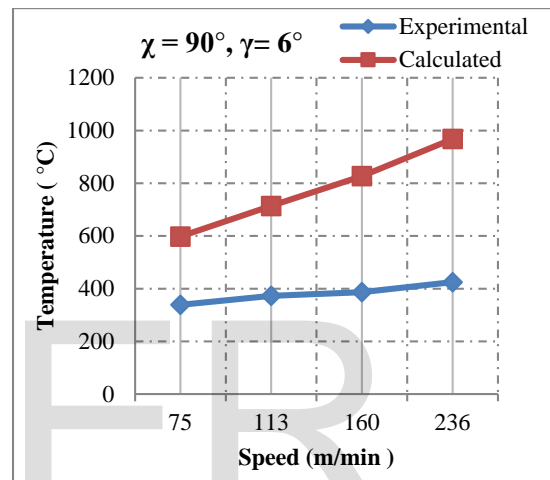


Fig.2 Experimental and calculated value for  $\chi = 90^\circ, \gamma = 6^\circ$

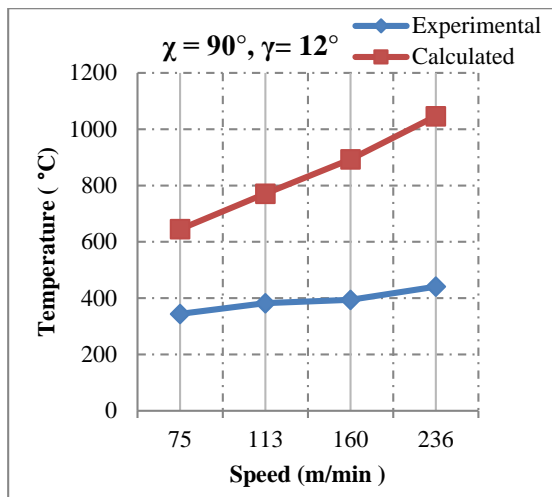


Fig.3 Experimental and calculated value for  $\chi = 90^\circ, \gamma = 12^\circ$

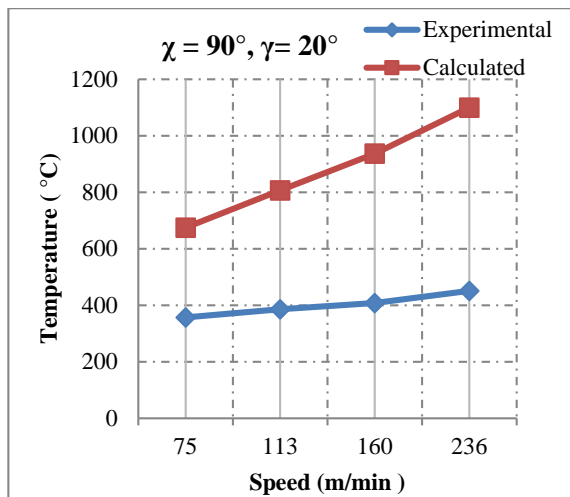


Fig.4 Experimental and calculated value for  $\chi = 90^\circ, \gamma = 20^\circ$

TABLE.1 EXPERIMENTAL AND CALCULATED VALUE OF TEMPERATURE AND FORCE COMPONENTS

Rake angle ( $\gamma$ )	Cutting edge angle( $\chi$ )	Temperature (°C experimental)	Temperature (°C calculated)	$F_c$ (N)	$F_f$ (N)	$F_t$ (N)	Feed (mm/rev)
6	45	474	986	318	102	123	0.16
		458	849	369	107	126	0.2
		394	727	437	110	126	0.25
		372	636	525	112	157	0.3
6	60	468	861	330	141	91	0.16
		415	738	386	150	92	0.2
		369	627	449	155	94	0.25
		355	544	474	158	120	0.3
6	75	441	799	320	143	58	0.16
		385	682	386	144	59	0.2
		357	576	450	145	61	0.25
		335	497	499	147	90	0.3
6	90	422	780	344	161	36	0.16
		375	665	388	142	44	0.2
		356	561	458	145	55	0.25
		333	482	490	161	78	0.3
12	90	451	818	325	143	26	0.16
		389	698	380	136	38	0.2
		364	589	440	135	46	0.25
		343	507	475	132	59	0.3
20	90	452	836	301	95	25	0.16
		390	716	376	96	36	0.2
		366	606	432	97	42	0.25
		344	523	465	99	53	0.3
0	90	394	724	363	438	622	0.16
		367	617	400	452	687	0.2
		343	520	464	479	689	0.25
		297	447	522	510	700	0.3
0	75	416	742	365	233	159	0.16
		370	633	453	250	188	0.2
		347	534	535	258	200	0.25
		325	461	577	267	230	0.3

TABLE.2

Rake angles	Cutting edge angle	v m/min	F <sub>c</sub> (N)	F <sub>f</sub> (N)	F <sub>t</sub> (N)	T °C (Exp)	T °C (Cal)
0	45	75	520	267	372	356	662
		113	491	252	341	384	798
		160	481	194	306	405	935
		236	456	159	216	452	1110
0	60	75	497	279	239	338	584
		113	480	247	210	367	700
		160	453	217	185	387	816
		236	423	172	111	421	962
0	75	75	490	344	190	333	544
		113	475	258	176	347	650
		160	448	233	150	380	754
		236	417	203	144	393	884
0	90	75	481	379	172	322	531
		113	474	341	163	344	634
		160	433	269	138	378	735
		236	410	271	118	392	860
6	45	75	456	194	132	380	745
		113	437	107	95	394	899
		160	419	95	78	443	1053
		236	406	60	58	474	1250
6	60	75	423	225	106	353	657
		113	411	147	82	383	788
		160	405	117	76	399	918
		236	398	111	48	448	1082
6	75	75	422	252	69	340	612
		113	409	177	56	374	731
		160	400	124	48	389	849
		236	395	69	44	431	995
6	90	75	416	288	57	339	598
		113	406	168	45	373	714
		160	400	144	43	387	827
		236	388	111	37	425	968
6	45	75	403	138	118	384	803
		113	398	118	105	428	969
		160	386	105	94	455	1136
		236	379	94	90	494	1349
12	60	75	396	150	92	368	709
		113	382	136	78	389	851
		160	376	118	72	428	991
		236	369	92	50	459	1169
12	75	75	393	164	56	354	660

		113	381	149	53	384	790
		160	372	142	49	397	917
		236	368	130	44	447	1075
12	90	75	386	168	46	344	645
		113	378	156	37	382	771
		160	371	154	33	394	893
		236	367	136	29	441	1046
12	45	75	368	104	93	388	838
		113	363	80	74	432	1012
		160	362	74	59	461	1187
		236	347	60	53	495	1411
20	60	75	363	107	83	378	740
		113	352	88	66	393	889
		160	342	83	63	437	1038
		236	324	71	58	473	1226
20	75	75	362	123	77	360	690
		113	351	115	69	388	827
		160	342	107	49	413	961
		236	319	82	41	453	1130
20	90	75	358	154	50	357	675
		113	345	144	44	386	807
		160	341	125	29	408	937
		236	302	98	24	451	1100

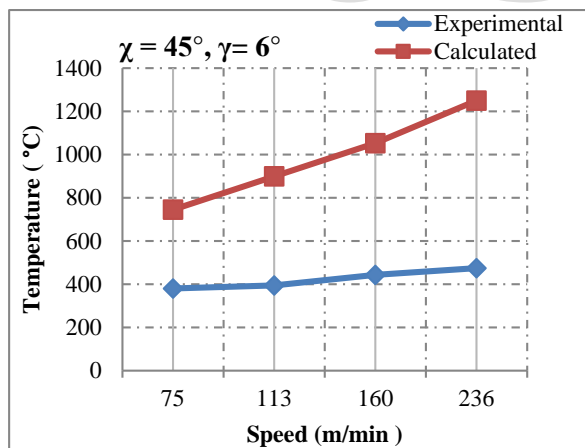


Fig. 5

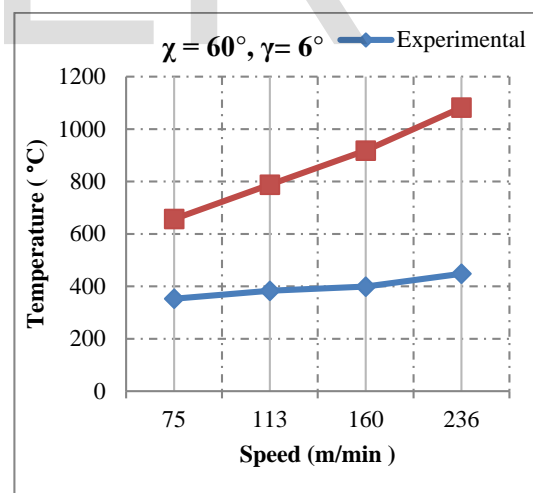


Fig.6

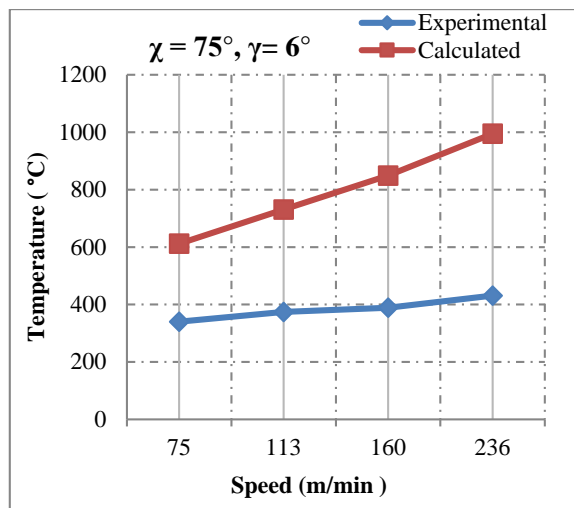


Fig.7 Temperature variation for,  $\chi = 75^\circ$ ,  $\gamma = 6^\circ$

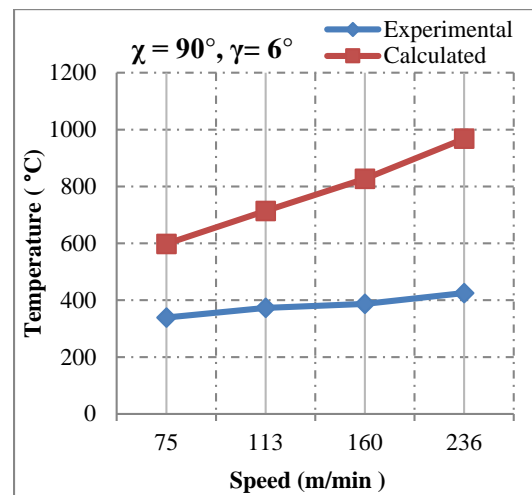


Fig.8 Temperature variation for,  $\chi = 90^\circ$ ,  $\gamma = 6^\circ$

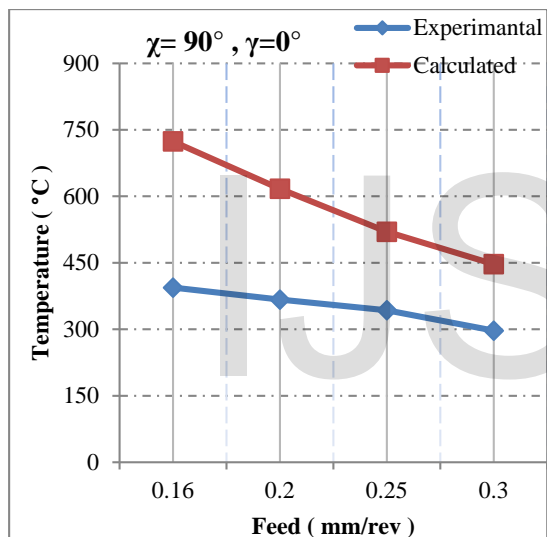


Fig.9 Temperature variation for,  $\chi = 90^\circ$ ,  $\gamma = 0^\circ$

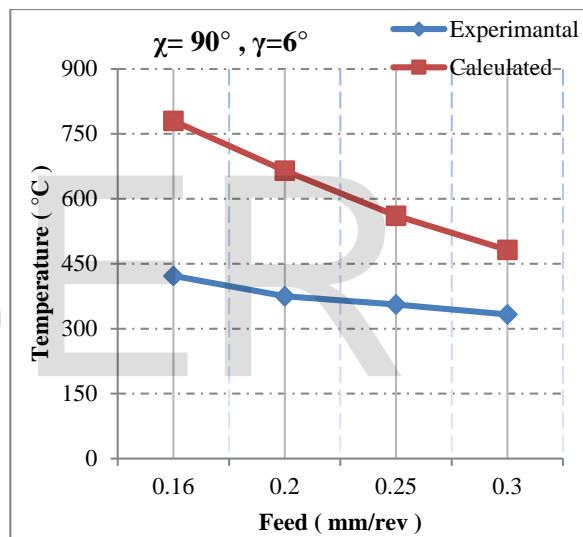


Fig.10 Temperature variation for,  $\chi = 90^\circ$ ,  $\gamma = 6^\circ$

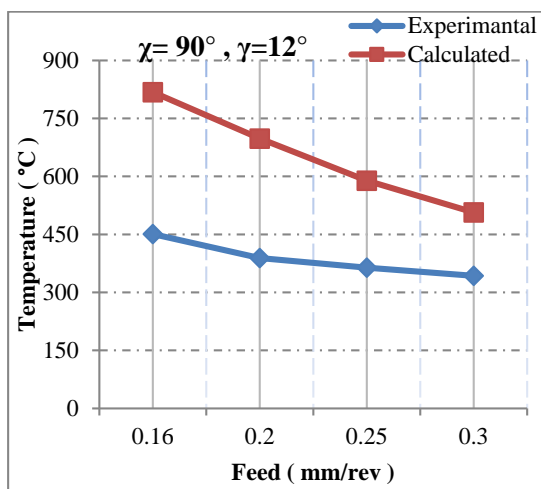


Fig.11 Temperature variation for,  $\chi = 90^\circ$ ,  $\gamma = 12^\circ$

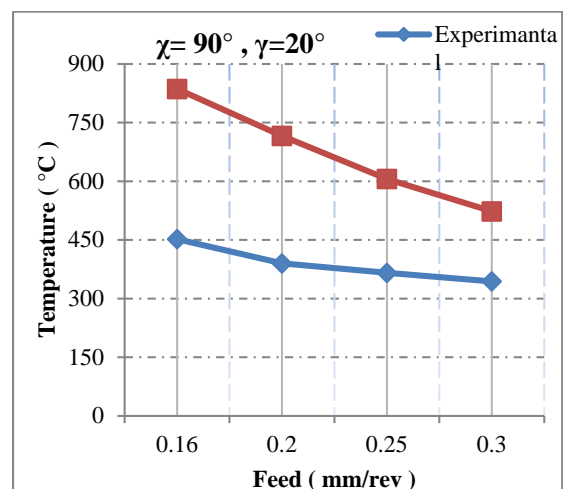


Fig.12 Temperature variation for,  $\chi = 90^\circ$ ,  $\gamma = 20^\circ$

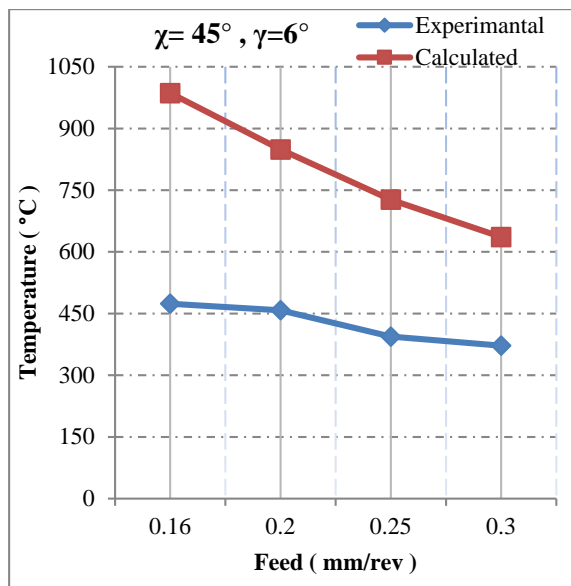


Fig.13 Temperature variation for,  $\chi = 45^\circ$ ,  $\gamma = 6^\circ$

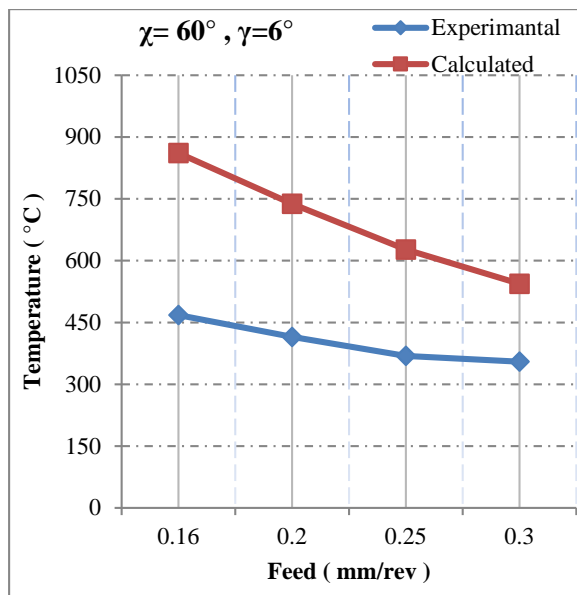


Fig.14 Temperature variation for,  $\chi = 60^\circ$ ,  $\gamma = 6^\circ$

Effect of feed on tool tip temperature for constant rake angle ( $\gamma = 6^\circ$ ) and different cutting edge angles ( $\chi = 45^\circ, 60^\circ, 75^\circ, 90^\circ$ ).

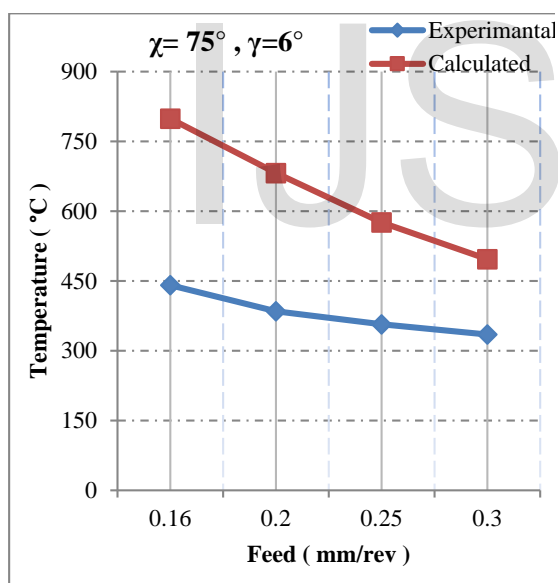


Fig.15 Temperature variation for,  $\chi = 75^\circ$ ,  $\gamma = 6^\circ$

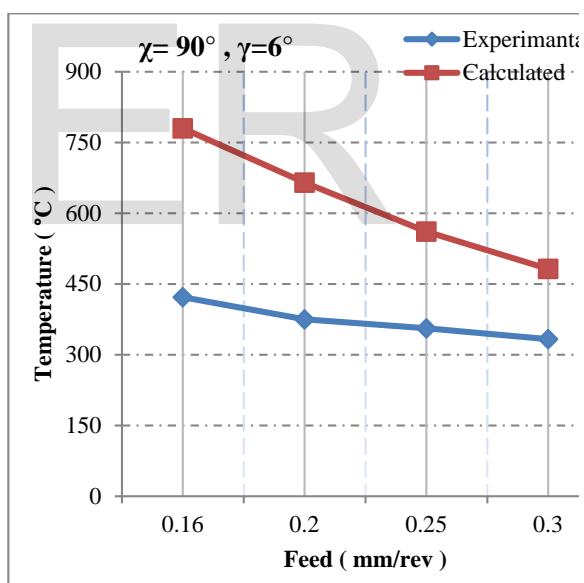


Fig.16 Temperature variation for,  $\chi = 90^\circ$ ,  $\gamma = 6^\circ$

## 2.3 Effect of Cutting Speed on Force Components

According to Fig 17 and 18 it has been observed that the value of components of forces decreases with increasing cutting speed.

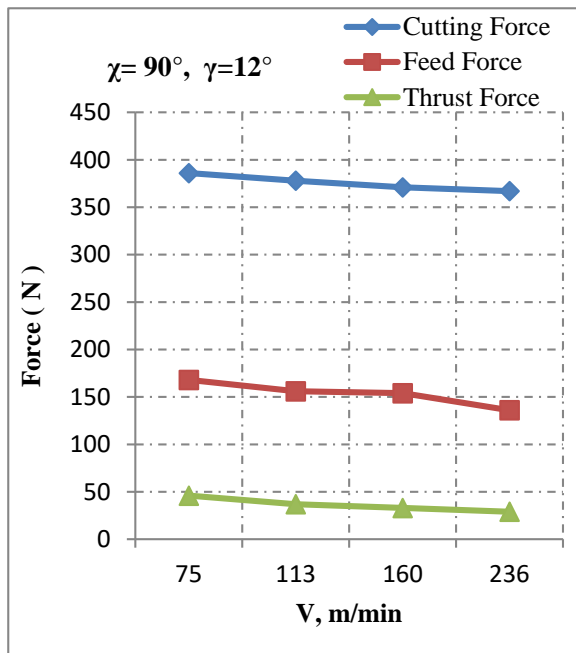


Fig.17 component of forces for,  $\chi = 90^\circ$ ,  $\gamma = 12^\circ$

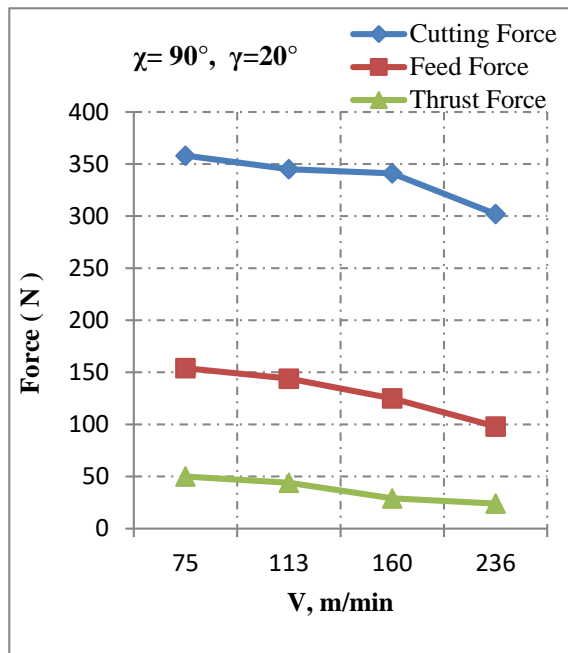


Fig.18 component of forces for,  $\chi = 90^\circ$ ,  $\gamma = 20^\circ$

Effects of variation of feed are shown in Fig.19 to 22, when value of cutting edge angle is constant ( $\chi = 90^\circ$ ) for different value of rake angle ( $0^\circ$ ,  $6^\circ$ ,  $12^\circ$ ,  $20^\circ$ ). According to graphs, it has been clear that with increasing feed rate, value of cutting force increases.

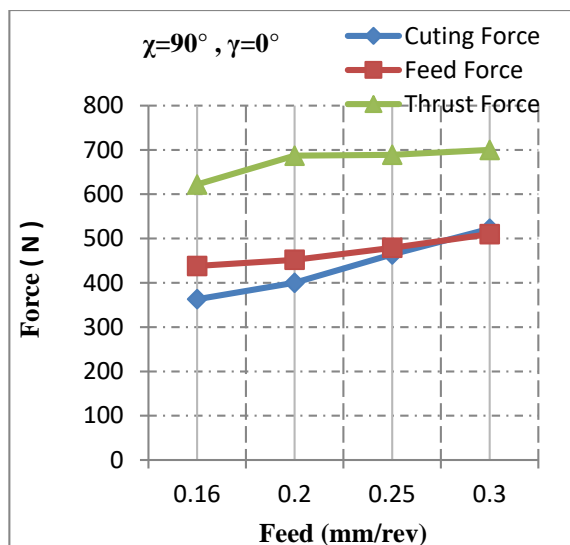


Fig.19 component of forces for,  $\chi = 90^\circ$ ,  $\gamma = 0^\circ$

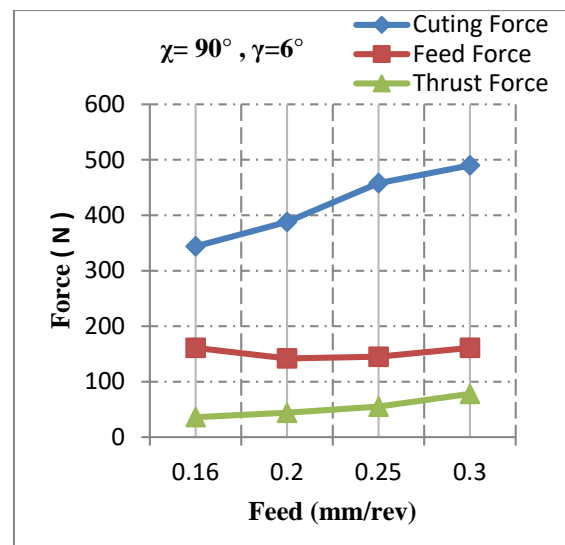


Fig.20 component of forces for  $\chi = 90^\circ$ ,  $\gamma = 6^\circ$



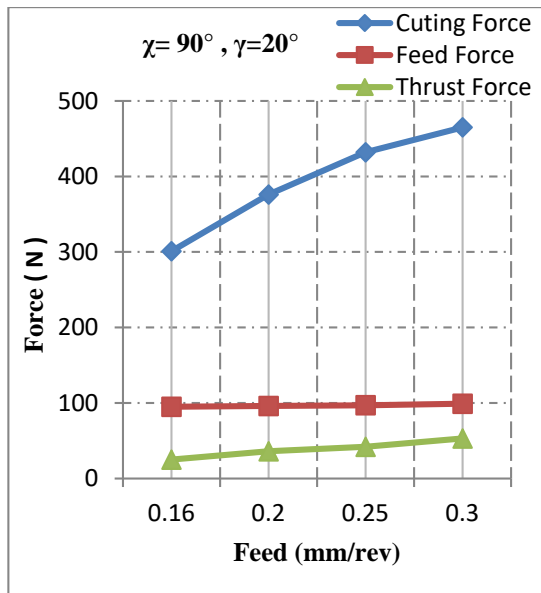


Fig.21 Component of forces for,  $\chi=90^\circ, \gamma=20^\circ$

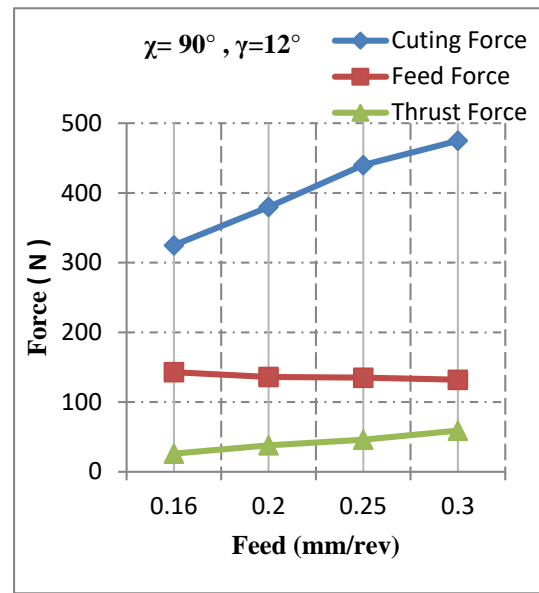


Fig.22 Component of forces for,  $\chi=90^\circ, \gamma=12^\circ$

## 4. CONCLUSIONS

### 4.1 Effects of speed and feed on tool tip temperature.

- Tool tip temperature increases with increasing cutting speed.
- Tool tip temperature decreasing with increasing feed rate this occurs due to decreasing machining time.
- Tool tip temperature also increases with increasing rake angle
- Tool tip temperature decreasing with increasing cutting edge angle.

### 4.2 Effects of speed and feed on cutting forces.

- Cutting forces always decreases with increasing cutting speed.
- Force components are proportional to the feed rate so feed force increases with increasing feed rate.

### 4.3 Effects of Cutting edge angle

- Magnitude of temperature increases with increasing cutting edge angle
- Force component decreases with increasing cutting edge angle.

### 4.4 Effects of Rake angle

- With increasing rake angle tool tip temperature decreases.
- With increasing rake angle force components decreases.

## REFERENCES

- [1] Saglam, Haci, Faruk Unsacar, and Suleyman Yaldiz. "Investigation of the effect of rake angle and approaching angle on main cutting force and tool tip temperature." International Journal of machine tools and manufacture 46.2 (2006): 132-141.
- 
- [2] Saglam, Haci, Suleyman Yaldiz, and Faruk Unsacar. "The effect of tool geometry and cutting speed on main cutting force and tool tip temperature." Materials & Design 28.1 (2007): 101-111.
-

5. [3] J.G. Lima, R.F. Avila, A.M. Abrão, M. Faustino, J.P. Davim, Hard turning: AISI 4340 high strength low steel and AISI D2 cold work tool steel, *J Mater Process Technol* 169 (2005) 388–395
- 6.
7. [4] Chou YK, Song H (2004) Tool nose radius effects on finish hard turning. *J Mater Process Technol* 148(2):259–268
- 8.
9. [5] Astakhov VP (2010) Geometry of single-point turning tools and drills. Fundamentals and practical applications. Springer, London
- 10.
11. [6] Bouacha K, Yallese MA, Mabrouki T, Rigal J (2010) Statistical analysis of surface roughness and cutting forces using response surface methodology in hard turning of AISI 52100 bearing steel with CBN tool. *J Refract Met Hard Mater* 28:349–361.
- 12.
13. [7] Kurt A, Seker U (2005) The effect of chamfer angle of polycrystalline cubic boron nitride cutting tool on the cutting forces and the tool stresses in finishing hard turning of AISI 52100 steel. *Mater Des* 26:351–356.
- 14.
15. [8] Aslan E, Camuscu N, Birgoren B (2007) Design optimization of cutting parameters when turning hardened AISI 4140 steel (63 HRC) with Al<sub>2</sub>O<sub>3</sub> + TiCN mixed ceramic tool. *Mater Des* 28:1618–1622.
- 16.
17. [7] Boothroyd G. Temperatures in orthogonal metal cutting. *Proc Inst Mech Engng* 1963;177:623–54.
- 18.
19. [8] Lazoglu I, Altintas Y. Prediction of tool and chip temperature in continuous and interrupted machining. *Int J Mach Tools Manufact* 2002;42:1011–22.

IJSER